FRIGID ZONE **MEDICINE**
Original Article • DOI: 10. 1515/fzm-2024-0017

Ethanol extract of cassia seed alleviates metabolic dysfunction-associated steatotic liver disease by acting on multiple lipid metabolism-related pathways

Wen Li[1#], Jia Wang[1#], YilianYang[1#], Chunlei Duan[1], Bing Shao[1], Mingxiu Zhang[1], Jiapan Wang[1], Peifeng Li[1], Ye Yuan[1], Yan Zhang[1], Hongyu Ji[1], Xingda Li[1], Zhimin Du[1,2*]

Abstract

Background and objective: In northern China's cold regions, the prevalence of metabolic dysfunction-associated steatotic liver disease (MASLD) exceeds 50%, significantly higher than the national and global rates. MASLD is an important risk factor for cardiovascular and cerebrovascular diseases, including coronary heart disease, stroke, and tumors, with no specific therapeutic drugs currently available. The ethanol extract of cassia seed (CSEE) has shown promise in lowering blood lipids and improving hepatic steatosis, but its mechanism in treating MASLD remains underexplored. This study aims to investigate the therapeutic effects and mechanisms of CSEE. **Methods:** MASLD models were established in male Wistar rats and golden hamsters using a high fat diet (HFD). CSEE (10, 50, 250 mg/kg) was administered *via* gavage for six weeks. Serum levels of total cholesterol (TC), triglyceride (TG), low-density lipoprotein cholesterol (LDL-C), high-density lipoprotein cholesterol (HDL-C), aspartate aminotransferase (AST), and alanine aminotransferase (ALT), as well as liver TC and TG, were measured using biochemical kits. Histopathological changes in the liver were evaluated using Oil Red O staining, Hematoxylin-eosin (H&E) staining, and transmission electron microscopy (TEM). HepG2 cell viability was assessed using the cell counting kit-8 (CCK8) and Calcein-AM/PI staining. Network pharmacology was used to analyze drug-disease targets, and western blotting was used to confirm these predictions. **Results:** CSEE treatment significantly reduced serum levels of TC, TG, LDL-C, ALT, and AST, and improved liver weight, liver index, and hepatic lipid deposition in rats and golden hamsters. In addition, CSEE alleviated free fatty acid (FFA)-induced lipid deposition in HepG2 cells. Molecular biology experiments demonstrated that CSEE increased the protein levels of p-AMPK, p-ACC, PPARα, CPT1A, PI3K P110 and p-AKT, while decreasing the protein levels of SREBP1, FASN, C/EBPα, and PPARγ, thus improving hepatic lipid metabolism and reducing lipid deposition. The beneficial effects of CSEE were reversed by small molecule inhibitors of the signaling pathways *in vitro*. **Conclusion:** CSEE improves liver lipid metabolism and reduces lipid droplet deposition in Wistar rats and golden hamsters with MASLD by activating hepatic AMPK, PPARα, and PI3K/AKT signaling pathways.

Keywords

cassia seed ethanol extract; metabolic dysfunction related fatty liver disease; network pharmacology

Received 28 June 2024, accepted 27 August 2024

[1]*Institute of Clinical Pharmacy, the Second Affiliated Hospital of Harbin Medical University (State Key Laboratory of Frigid Zone Cardiovascular Diseases), Harbin 150086, China.*
[2]*State Key Laboratory of Quality Research in Chinese Medicines, Macau University of Science and Technology, Macau 999078, China.*

**Corresponding author Zhimin Du, E-mail: dzm1956@126.com*
[#]These authors made equal contributions to this work.

1 Introduction

With changes in dietary habits, work styles, and the global rise in obesity and type 2 diabetes mellitus (T2DM)[1], the incidence of metabolic dysfunction-associated steatotic liver disease (MASLD) has been gradually increasing. MASLD has now become the leading chronic liver disease and a significant public health issue worldwide[2-3]. It has been observed that residents in high-altitude and cold regions experience severe dietary imbalance[4]. In addition to insulin resistance, dyslipidemia, hypertension, and mitochondrial

dysfunction[5-8], cold weather is an independent risk factor for the development of fatty liver disease and contributes to the higher prevalence of MASLD[9]. In northern China's cold regions, MASLD prevalence exceeds 50%, significantly surpassing national and global rates. The cold environment is known to significantly impact various energy metabolism processes in animals and is linked to metabolic diseases[10-11]. Consequently, managing MASLD poses an even greater challenge for patients residing in these cold regions.

Lifestyle interventions, including dietary modifications and increased physical activity, remain the primary treatment for MASLD[12]. Drug therapy may be considered for patients' who struggle to adhere to a healthy lifestyle or when the disease progresses to more severe stages, such as metabolic-associated steatotic hepatopathy (MASH). To date, the only one approved medication for t MASLD is Resmetirom, an oral selective thyroid hormone receptor (THR)-β agonist[13]. The complex pathogenesis of MASLD, combined with the limitations of existing drugs in managing disease progression, underscores the need for the development of highly effective and low-toxicity treatment options.

Cassia seed, derived from the mature seeds of Cassia obtusifolia or Cassia tora, is widely distributed across various provinces in China. It contains anthraquinones, naphthopyranones, flavonoids, terpenoids, fatty acids, and polysaccharides, with anthraquinones being the most predominat[14]. Clinically, Cassia seed is used for treating eye diseases, neurological disorders, hypertension, hyperlipidemia, and diabetes mellitus[15-19]. Moreover, cassia seed has demonstrated hepatoprotective effects. The orange cassia pigment isolated from cassia seed induces AMP-activated protein kinase (AMPK) phosphorylation, which activates transcription factor EB (TFEB) and promotes autophagic flux, thereby alleviating hepatic steatosis induced by a high-fat and high-fructose diet[20]. Changes in intestinal flora are known to significantly impact hepatic health[21], and cassia seed extract has been shown to protect against high-fat diet-induced hepatic injury in mice by ameliorating intestinal barrier function and promoting intestinal flora homeostasis[22]. However, variations in extraction methods and processes can alter the composition of Chinese medicines, potentially leading to different therapeutic effects. Given the complexity of its components and their multiple targets, we investigated the effects of 90% ethanol-extracted cassia seed on MASLD and explored the potential mechanisms underlying its hepatoprotective effects.

2 Materials and methods

2.1 Chemicals and reagents

Cassia extract was provided by the Department of Natural Medicinal Chemistry, Harbin Medical University. The extraction process involved initial extraction with 70% ethanol, followed by treatment with microporous resin and elution with 90% ethanol. The content of total anthraquinone compounds in the extract is detailed in Supplementary Table 1. The high-fat diet (HFD) used in this study was supplied by Huafukang Bio-technology Co., Ltd (Beijing, China) under license No. SCXK (Beijing) 2019-0008. The HFD composition includes Casein 25.84%, L-cystine 0.39%, maltodextrin 16.15%, sucrose 8.89%, cellulose 6.46%, soybean oil 3.23%, lard 31.66%, minerals 1.29%, DiCalcium phosphate 1.68%, calcium carbonate 0.72%, potassium citrate 2.13%, choline bitartrate 0.26%, vitamins 1.29%, and dye 0.01%.

2.2 Animals maintenance and experiments

All experimental animal protocols were approved by the Ethics Committee of the Second Affiliated Hospital of Harbin Medical University (SYDW2019-258). Specific pathogen-free (SPF) male wistar rats (180-200 g) and male golden Syrian hamsters (110-130g) were purchased from Changsheng Biotechnology (Liaoning, China) under license number SCXK (Liao) 2020-0001. Animals were housed in a standard environment (temperature 23 ± 1°C, humidity of 55 ± 5%) with a 12:12-hour light-dark cycle, and were provided with a normal diet (ND) and free access to water. After one week of acclimatization, they were randomly assigned to experimental groups. Animal models of MASLD were constructed by feeding the rats a HFD for four weeks and the hamsters for 25 days[23-24]. The HFD-fed animals were then randomly divided into a model group and ethanol extract of cassia seed (CSEE) treatment groups (10, 50, 250 mg/kg), with treatments administered *via* gavage for six weeks.

2.3 Serum and liver biochemical indicators assay

After successfully constructing the MASLD model, 1-1.5 ml of blood was collected *via* orbital blood sampling. Blood samples were placed on ice for 30 min, then centrifuged at 3000 rpm for 10 min at 4°C. The serum was transferred to new centrifuge tubes and analyzed immediately or stored at -80°C for later use. Serum total cholesterol (TC, A111-1-1), triglyceride (TG, A110-1-1) , and low-density lipoprotein cholesterol (LDL-C, A113-1-1) were measured at 500 nm and 600 nm, respectively, while alanine aminotransferase (ALT, C009-2-1) and aspartate aminotransferase (AST, C010-2-1) were measured at 510 nm using biochemical kits from Jiancheng Biotechnology Co., China..

Liver tissues were rapidly dissected and frozen in liquid nitrogen. About 20 mg of liver tissue from the same lobe was homogenized with lysate, centrifuged at 2500 rpm for 10 min, and the supernatant was used to determine TC and TG content. The samples were either analyzed immediately or stored at -80°C for future use.

2.4 Histopathological analysis

Liver tissues were fixed in 4% paraformaldehyde for 24 h. Subsequently, the tissues were dehydrated through a gradient of ethanol and xylene, embedded in paraffin wax, and sectioned into 5-μm slices. Morphological changes in the liver were examined using Hematoxylin and eosin (H&E) staining (G1120, Solarbio, Beijing, China). Additionally, another portion of the liver was dehydrated using a 30% sucrose solution, embedded in optimal cutting temperature (O.C.T.) compound (SAKURA Tissue-Tek®), and sectioned into 10-μm slices. Lipid deposition of the liver was assessed using Oil Red O staining (G1261, Solarbio, Beijing, China).

2.5 Transmission electron microscopy (TEM)

Tissue blocks of approximately 1 mm3 were extracted from the same liver location in each experimental group and fixed d in 2.5% glutaraldehyde solution for 48 h. The blocks were then stained with 4% cobalt acetate solution for 30 min, followed by dehydration through a gradient of ethanol. The samples were embedded in a mixture of anhydrous acetone andf embedding agent for 2 h, then polymerized in an oven at 37°C for 24 h and at 60°C for 48 h. Finally, the samples were stained with uranyl acetate and lead citrate, and the tissue ultrastructure was examined using TEM.

2.6 Cell culture and treatment

HepG2 cells were cultured in Dulbecco modified Eagle medium (DMEM, Sigma, USA) supplemented with 10% fetal bovine serum (FBS, Bioind, Israel) and 5% penicillin and streptomycin (Seven, China). The cells were maintained in a water-saturated atmosphere of 95% air and 5% CO2 at 37°C. For the experiments, the cells were exposed to free fatty acid (FFA) at a concentration of 250 μmol/L for 24 h. Subsequently, the cells were treated with CSEE at concentrations of 0.1, 1, 10 μg/mL for 24 h. Additionally, specific signal pathway inhibitors (Compound C/GW6471/LY294002, MCE, USA) were pre-treated 4 h before the CSEE (10 μg/mL) treatment to evaluate the effect of CSEE. At the end of the experiments, the cells were harvested for further analysis.

2.7 Cell viability assay

Cell counting kit-8 (CCK8, Seven, China) and a Calcein-AM/propidium iodide (Calcein-AM/PI) cell activity and cytotoxicity assay kit were used to assess the effect of CSEE on cell activity. HepG2 cells, grown to an appropriate density in 96-well plates, were treated with CSEE for 24 h. After treatment, 10 μL of CCK8 solution was added to each well, and the cells were incubated in the culture incubator for approximately 2 h. Absorbance was measured at 450 nm using a Tecan Infinite M200PRO Multimode Plate Reader (Switzerland) to calculate cell viability. For the Calcein AM/PI assay, the working solution was prepared according to the instructions and added to the cell culture plates. The samples were incubated at 37°C for 30 min, protected from light. Images were acquired using a laser scanning confocal microscope (Olympus, Fluoview1000, Tokyo, Japan), and the ratio of dead to live cells was determined based on fluorescence intensity.

2.8 Nile red staining

Cells were fixed with 4% paraformaldehyde for 20 min at room temperature. Following fixation, cells were washed with PBS buffer. Nile red dye working solution was then added according to the manufacturer's instructions and incubated for 10 min at room temperature, protected from light. DAPI staining solution was subsequently added to each well and incubated for 10 min, also protected from light. Intracellular lipid deposition was observed and quantified using a laser scanning confocal microscope, with analysis based on fluorescence intensity.

2.9 Screening of the targets of MASLD

The Gene Expression Omnibus (GEO) database (https://www.ncbi.nlm.nih.gov/geo/) was used to identify gene expression datasets related to MASLD. The search criteria included “MASLD” and “NAFLD”[25]. The dataset GSE135251, which comprises 206 patient samples and 10 control samples, was selected for analysis. GEO2R was used to visualize the data with volcano plots and heat maps. The Bioinformatics website (http://www.bioinformatics.com.cn/) was employed to further enhance these visualizations. Potential therapeutic targets for MASLD were predicted using several databases: GeneCards (https://www.genecards.org/), DisGeNET (https://www.disgenet.org/), MalaCards (https://previous.malacards.org/pages/info), the Comparative Toxicogenomics Database (CTD) (https://ctdbase.org/), and OMIM (https://www.omim.org/). The predicted therapeutic targets were then cross-referenced with the dataset GSE135251. Targets that appeared at least three times were selected for further study and were also standardized using the UniProt database.

2.10 Screening and analysis of drug-disease common targets

Livers from hamsters in the HFD group and those gavage-administered CSEE (250 mg/kg) were subjected to high-throughput sequencing to identify differential genes. Overlapping differential genes with \ MASLD therapeutic targets were analyzed using Venn diagrams on the bioinformatics website (http://www.bioinformatics.com.cn/). The 30 selected targets were uploaded to the

STRING 12.0 (https://cn.string-db.org/) to construct protein-protein interaction (PPI) networks. Data visualization and network topology analysis were performed using Cytoscape 3.10.1, with hub genes further identified using Cytohubba and MCODE plugins.

Gene Ontology (GO) and Kyoto Encyclopedia of Genes and Genomes (KEGG) enrichment analyses for the 30 targets were visualized on the bioinformatics website (http://www.bioinformatics.com.cn/). GO analysis covered three ontologies: biological process (BP), molecular function (MF), and cellular component (CC). The top 20 GO terms and top 50 KEGG pathways were displayed.

2.11 Molecular docking

The SDF structure of CSEE active ingredient was obtained from PubChem (https://pubchem.ncbi.nlm.nih.gov/) and converted to mol2 format using OpenBabel 2.4.1. Hydrogenation was performed in Autodock Vina, and the file was exported to pdpqt format. The PDB structure of the receptor protein, was sourced from UniProt, filtered based on resolution and publication date. Dehydration and hydrogenation of the receptor were done in Autodock Vina, and the resulting pdbqt files were prepared. Both ligand and receptor pdbqt files were then imported into Autodock Vina for molecular docking.

2.12 Western blot

Total protein samples from liver tissues of rats and hamsters were extracted using RIPA buffer (Beyotime, China) supplemented with protease inhibitors (Roche, Germany). Protein concentrations were measured using a BCA protein detection kit (Beyotime, Shanghai, China). The proteins were then separated by 7.5% or 10% SDS-PAGE and transferred to nitrocellulose membranes. After blocking with a rapid blocking solution, the membranes were incubated with primary antibodies at 4°C overnight. The following primary antibodies were used: β-Actin (TA-09, 1：1000, ZSGB Co. Ltd, China), PPARα (A18252, 1：1000, ABclonal, China), PPARγ (16643-1-AP, 1：1000, Proteintech, China), Carnitine Palmitoyltransferase 1A (CPT1A) (15184-1-AP, 1：1000, Proteintech, China), Fatty Acid Synthase (FASN) (10624-2-AP, 1：1000, Proteintech, China), CCAAT/Enhancer Binding Protein α (C/EBPα) (18311-1-AP, 1：1000, Proteintech, China), p-AMPKα (CY5608, 1：1000, Abways, China), AMPKα1 (bsm-33338M, 1：1000, Bioss, China), p-Acetyl CoA Carboxylase (p-ACC) (11818T, 1：1000, Cell Signaling Technology, USA), ACC (3676T, 1：1000, Cell Signaling Technology, USA), PI3K/AKT (AF5112, 1：1000, Affinity, China), p-AKT (AF0016, 1：1000, Affinity, China), AKT (AF6261, 1：1000, Affinity, China), and Sterol Regulatory Element-Binding Protein 1 (SREBP1) (ab28481, 1：1000, Abcam, UK).

Following primary antibody incubation, the membranes were washed with PBS-Tween (0.5%) and then incubated with secondary antibodies at room temperature for 1 hour. The secondary antibodies used were goat anti-mouse IgG (P/N 926-32210, LI-COR Biosciences, USA) and goat anti-rabbit IgG (P/N 926-32211, LI-COR Biosciences, USA). Finally, blot band images were captured using an imaging system (LI-COR Biosciences, USA).

2.13 Real-time PCR (RT-PCR)

Total RNA was extracted from liver tissues of rats and hamsters using TRIZOL reagent (Invitrogen, Carlsbad, CA) following the manufacturer's protocol. RNA concentration was measured with a Nanodrop 2000 microspectrophotometer (Thermo Fisher Scientific), and then reverse-transcribed into complementary DNA using the ReverTra Ace qPCR RT Kit (Toyobo, Japan). Quantitative mRNA expression was assessed with an LC480 Real-time PCR system (Roche, USA) and SYBR Green PCR Master Mix (Roche, USA). The 18S rRNA gene was used as an internal control, and gene expression levels were calculated using the $2^{-\Delta\Delta Ct}$ method. The primers used in this study are listed in Supplementary Table 2.

2.14 Statistical analysis

GraphPad Prism 9.0 was used for data analysis. The experimental data are presented as the mean ± SEM. Statistical comparisons were made using one-way analysis of variance (ANOVA) followed by a post hoc Tukey test for multiple group comparisons. Statistical significance was defined as a P-value < 0.05.

3 Results

3.1 CSEE inhibits HFD-induced elevation of serum lipid and transaminase levels in rats with MASLD

An animal model of HFD-induced MASLD was established, and CSEE was administered orally for 6 weeks. The experimental flow is illustrated in Fig. 1A. Serum lipid changes in rats fed an HFD for four weeks are shown in Supplementary Fig. 1. Following successful model establishment, the effects of CSEE (10, 50, and 250 mg/kg) on serum lipid and transaminase levels were evaluated. As shown in Fig. 1B, CSEE (50 and 250 mg/kg) effectively inhibited chylomicronemia induced by HFD. Figures 1C, D, E, and F demonstrate that CSEE (50 and 250 mg/kg) significantly reduced serum levels of TC, TG, and LDL-C but had no effect on HDL-C. In addition, Fig. 1G and 1H indicates that CSEE (50 and 250 mg/kg) significantly inhibited the elevation of serum ALT and AST levels induced by HFD.

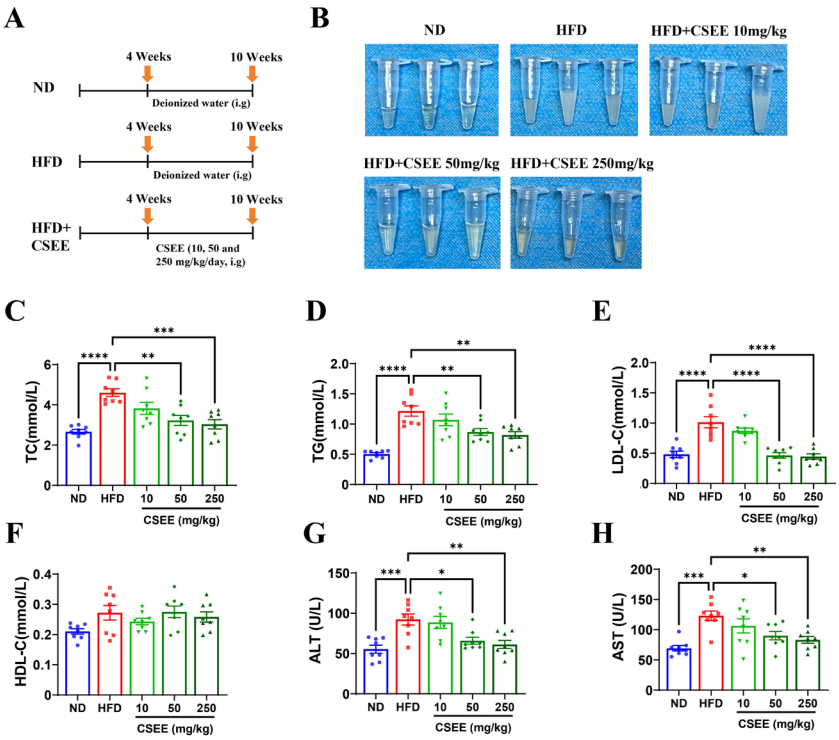

Fig. 1 Cassia seed ethanol extract (CSEE) reduces elevated blood lipids and serum transaminase in rats fed with high-fat diet (HFD)

(A) Diagram illustrating the rat-feeding timeline. (B) Appearance of rat serum samples, $N = 3$. (C-H) Serum levels of (C) total cholesterol (TC), (D) triglyceride (TG), (E) low-density lipoprotein cholesterol (LDL-C), (F) high-density lipoprotein cholesterol (HDL-C), (G) alanine aminotransferase (ALT), and (H) aspartate aminotransferase (AST), measured in rats after CSEE oral administration for 6 weeks, $N = 8$ per group. $^{*}P < 0.05$, $^{**}P < 0.01$, $^{***}P < 0.001$, $^{****}P < 0.0001$. ND: Normal Diet.

3.2 CSEE inhibits HFD-induced hepatic steatosis in rats with MASLD

Hepatic steatosis is a key clinical feature of MASLD[26]. Therefore, we investigated the effects of CSEE on liver lipid deposition in MASLD rats. Firstly, we assessed the morphological changes in liver samples from each group. Fig. 2A shows that livers from the ND group had a dark red color, smooth surface, and elastic texture. In contrast, livers from the HFD group were noticeably paler, larger, and slightly firmer. Treatment with CSEE (50 and 250 mg/kg) ameliorated the morphological changes induced by HFD, suppressing the increase in liver volume. We also examined the effects of CSEE on liver weight and liver index (the weight ratio of liver and body). Fig. 2B, C, and D shows that rats in the HFD group had significantly higher body weight, liver weight, and liver index compared to the ND group. Although CSEE administration did not affect the body weight of HFD-induced rats, it did reduce liver weight and liver index in MASLD rats at doses of 50 and 250 mg/kg. Additionally, we assessed the lipid content in the livers of rats from each experimental group. Fig. 2E and F demonstrate that CSEE (50 and 250 mg/kg) effectively inhibited the increase in liver TC and TG levels induced by HFD.

Histopathological staining was used to observe lipid changes in the live. H&E staining in results Fig. 2G revealed that hepatocytes in the ND group were regularly arranged with normal structure, showing no apparent inflammatory infiltration or lipid droplet accumulation. In contrast, the liver tissue from the HFD group exhibited severe steatosis, characterized by numerous irregular fat vacuoles within the cytoplasm, swollen hepatocytes, and nuclei displaced to the cell peripheries. These pathological changes were significantly ameliorated by CSEE (50 and 250 mg/kg). Oil Red O staining results in Fig. 2H corroborated the findings from H&E staining. The HFD group displayed pronounced red lipid droplet aggregation, whereas CSEE (50 and 250mg/kg) improved lipid droplet accumulation in MASLD rats. These observations were further validated by TEM in Fig. 2I, which shows that CSEE (50 and 250 mg/kg) inhibited hepatic lipid deposition and reduced both the volume and number of lipid droplets in the livers of MASLD rats.

3.3 CSEE inhibits HFD-induced elevation of serum lipid and transaminase levels in golden Syrian hamsters with MASLD

We have confirmed that CSEE has therapeutic effects on HFD-induced hyperlipidemia and hepatic steatosis in rats with MASLD.

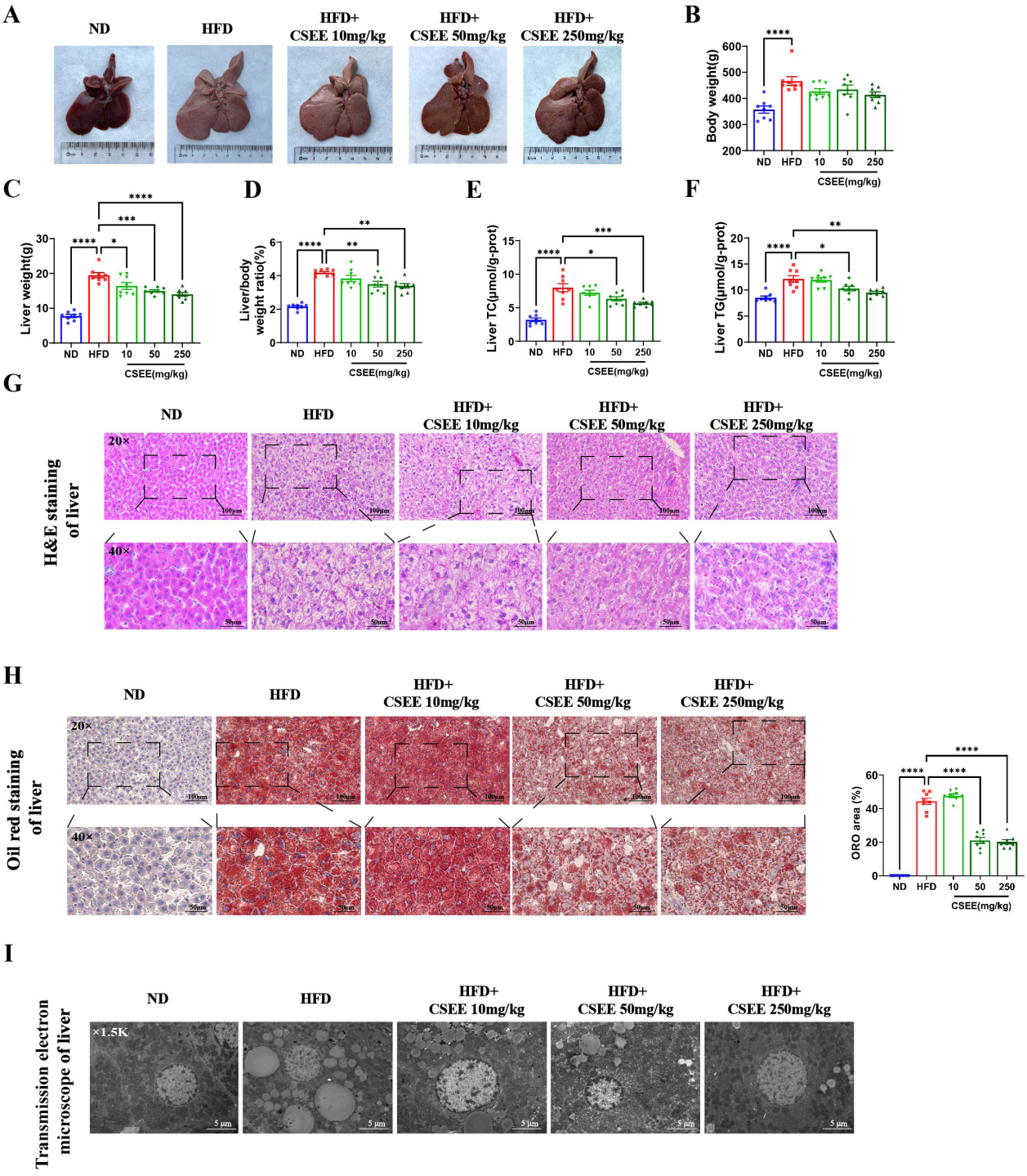

Fig. 2 Cassia seed ethanol extract (CSEE) prevents high-fat-diet (HFD) feeding-induced hepatic morphological changes and lipid deposition in rats

(A) Representative images of rat livers from various groups. (B) Body weight, $N = 8$ per group. (C) Liver weight, $N = 8$ per group. (D) The weight ratio of liver and body, $N = 8$ per group. (E-F) Liver (E) total cholesterol (TC), and (F) triglyceride (TG) contents of rats from various groups, $N = 8$ per group. (G) Hematoxylin-eosin (H&E) staining of rat liver tissues. (H) Oil Red O staining of rat liver tissues. Scale bar: 100 μm; 50 μm, $N = 8$ per group. (I) Representative electron microscopic images of rat liver tissue slices from various groups. Scale bar: 5 μm. $^{*}P < 0.05$, $^{**}P < 0.01$, $^{***}P < 0.001$, $^{****}P < 0.0001$. ND: Normal diet.

To ensure the reliability and reproducibility of these effects, as outlined in the technical guidelines for new drug studies, it is important to evaluate CSEE in a different animal model. Thus, we investigated the effects of CSEE in golden Syrian hamsters with MASLD. Previous studies established that feeding a HFD for 25 days leads to hyperlipidemia and hepatic steatosis in hamsters[24]. Fig. 3A provides a schematic of the hamster feeding process, and blood lipid levels at 25 days are shown in Supplementary Fig. 2. Fig. 3B-F indicates that continuous HFD feeding induces hyperlipidemia in hamsters. However, CSEE administered by gavage at doses of 10, 50, and 250 mg/kg for six weeks improved HFD-induced alterations in serum lipid levels, in hamsters, although it effectively reduced serum ALT and AST levels. The 50 mg/kg dose of CSEE did not affect serum TG, ALT, or AST levels in hamsters, which may be attributed to e differences in lipid metabolism between rats and hamsters. This suggests that a higher dose of CSEE may be required to effectively treat hyperlipidemia in MASLD hamsters.

3.4 CSEE inhibits HFD-induced hepatic steatosis in golden Syrian hamsters with MASLD

Next, we went on to evaluate the effect of CSEE on hepatic steatosis in hamsters. The livers from the HFD group appeared lighter in color and slightly larger than those from the ND group. CSEE (250 mg/kg) alleviated these HFD-induced morphological alterations in the liver of hamsters (Fig. 4A). Unlike the results observed in rats, there was no significant change in the body weight of hamsters after HFD feeding (Fig. 4B). This lack of change might be attributed to differences in intake and lipid metabolism between hamsters and rats, consistent with previous findings[24]. Liver weight and liver index were significantly higher in the HFD group compared with the ND group (Fig. 4C and D). Treatment with CSEE (50, 250 mg/kg) for six weeks reduced liver weight and liver index in hamsters. We further analyzed liver lipid content across all groups. Fig. 4E and F show that CSEE (250 mg/kg) effectively inhibited the HFD-induced increase in TC and TG levels in the liver. However, the 50 mg/kg dose of CSEE did not significantly improve hepatic lipid deposition, which may be related to the more advanced progression of MASLD in hamsters compared to rats.

We then analyzed the histopathological staining of hamster liver tissues from each group. H&E staining results in Fig. 4G indicated that CSEE (250 mg/kg) improved HFD-induced hepatic tissue steatosis by reducing hepatocyte swelling and the number of fat vacuoles. Similarly, Oil Red O staining in Fig. 4H demonstrated that CSEE (250 mg/kg) effectively inhibited the accumulation of

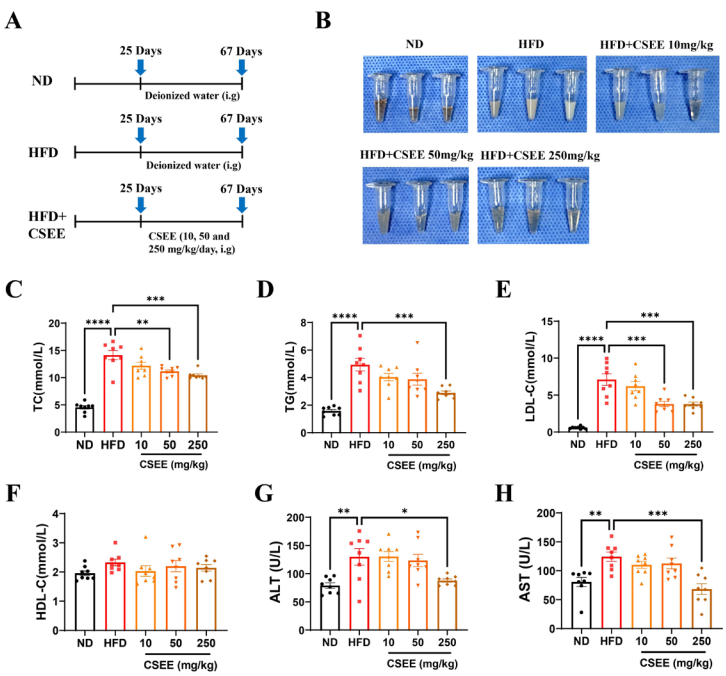

Fig. 3 Cassia seed ethanol extract (CSEE) reduces elevated blood lipids and serum transaminase in hamsters fed with high fat diet (HFD)

(A) Diagram illustrating the feeding timeline for hamsters. (B) Appearance of hamster serum samples, $N = 3$. (C-H) Serum levels of (C) total cholesterol (TC), (D) triglyceride (TG), (E) low-density lipoprotein cholesterol (LDL-C), (F) high-density lipoprotein cholesterol (HDL-C), (G) alanine aminotransferase (ALT), and (H) aspartate aminotransferase (AST), measured in hamsters after CSEE oral administration for 6 weeks, $N = 8$ per group. $^{*}P < 0.05$, $^{**}P < 0.01$, $^{***}P < 0.001$, $^{****}P < 0.0001$. ND: Normal diet.

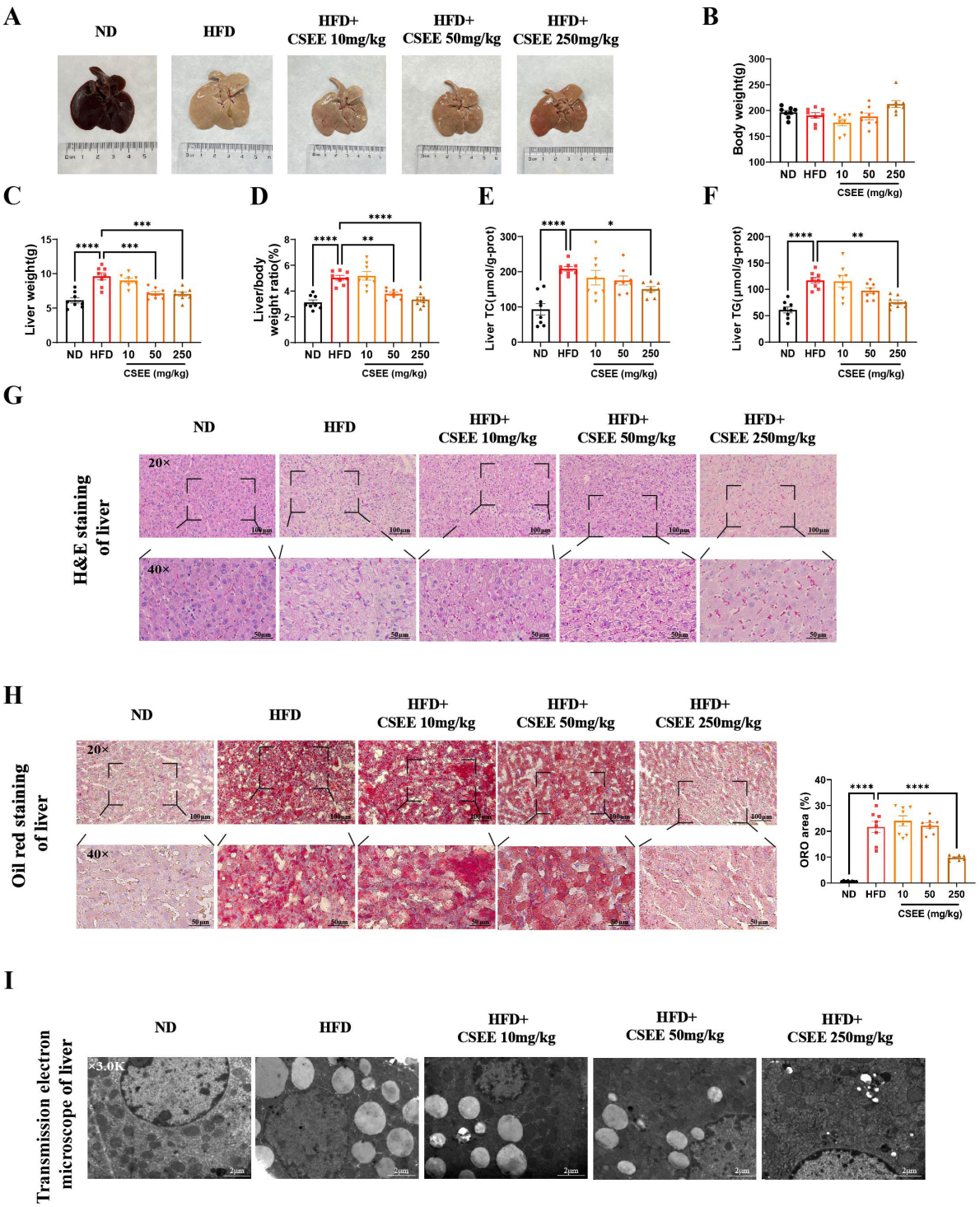

Fig. 4 Cassia seed ethanol extract (CSEE) prevents high-fat-diet (HFD) feeding-induced hepatic morphological changes and lipid deposition in hamsters

(A) Representative images of hamster livers from different groups. (B) Body weight, $N = 8$ per group. (C) Liver weight, $N = 8$ per group. (D) The weight ratio of liver and body, $N = 8$ per group. (E-F) Liver (E) total cholesterol (TC), and (F) triglyceride (TG) contents in hamsters of different groups, $N = 8$ per group. (G) Hematoxylin-eosin (H&E) staining of hamster liver tissues. (H) Oil Red O staining of hamster liver tissues. Scale bar: 100 μm; 50 μm, $N = 8$ per group. (I) Representative electron microscopic images of hamster livers of various groups. Scale bar: 2 μm. $^{*}P < 0.05$, $^{**}P < 0.01$, $^{***}P < 0.001$, $^{****}P < 0.0001$. ND: Normal diet.

lipid droplets in the liver. These findings were further corroborated by the observation of liver ultrastructure in Fig. 4I, which was consistent with the above results.

3.5 CSEE inhibits FFA-induced lipid accumulation in HepG2 cells

To further elucidate the role of CSEE, we conducted *in vitro* studies using HepG2 cells. The effects of CSEE on cell proliferation and viability were determined using Calcein-AM/PI staining and CCK8 assay. Fig. 5A and 5B demonstrates that CSEE concentrations ranging from 0.1 to 10 μg/mL did not affect HepG2 cell viability, whereas a concentration of 100 μg/mL of CSEE induced apoptosis *in vitro*. To avoid potential interference with cell viability in subsequent experiments, we selected CSEE doses of 0.1-10 μg/mL to investigate its effects on cellular lipid deposition.

We used FFA at a concentration of 250 μmol/L to induce intracellular lipid deposition in HepG2 cells and treated the cells with CSEE for 24 h to observe changes in intracellular lipid levels. Fig. 5C and 5D reveals that FFA treatment significantly increased intracellular levels of TC and TG. However, treatment with 10 μg/mL of CSEE reduced the TC and TG content in the cell.

Finally, Oil Red O staining was used to assess the deposition of intracellular lipid droplets in HepG2 cells. Fig. 5E shows that lipid droplets were significantly increased after 24 h of FFA treatment. However, 10 μg/mL of CSEE reduced the aggregation of these lipid droplets, while the other two concentrations of CSEE had no effect on lipid droplet formation. Additionally, Nile Red staining was used to further evaluate intracellular lipid deposition. The results, shown in Fig. 5F, were consistent with those obtained from Oil Red O staining, confirming the inhibitory effect of 10 μg/mL of CSEE on lipid droplet accumulation.

3.6 Prediction and analysis of targets related to MASLD and CSEE

To further explore the mechanism underlying the pharmacological effects of CSEE, we used network pharmacology for prediction and analysis. Initially, we identified therapeutic targets for MASLD. Given that MASLD is a relatively recent reclassification of NAFLD, data related to NAFLD remains relevant for MASLD research[25]. Consequently, we used “NAFLD” as a keyword to search the GEO database. We selected the GSE135251 dataset, which includes 10 normal liver tissues and 206 liver tissues from patients. We predicted the disease-related targets using several databases: GeneCards, DisGeNET, MalaCards, CTD, and OMIM. These predicted targets were then compared with differentially expressed genes (DEGs) from the GSE135251 dataset. The overlap of these targets was visualized using venn diagrams, as shown in Fig. 6A. Targets that appeared in at least three of the sources were selected, resulting in 673 targets for further analysis. High-throughput sequencing was conducted to analyze liver samples from the HFD group and the CSEE (250 mg/kg) group in hamsters. As shown in the volcano plot in Fig. 6B, the threshold of fold change and *P*-value were set at 1.5 and 0.05, respectively. This analysis identified a total of 668 DEGs, comprising 363 down-regulated genes and 305 up-regulated genes. To facilitate the understanding of the functions and biological processes associated with these DEGs, we performed GO enrichment and KEGG pathway analysis. The results of these analyses are presented in Supplementary Fig. 3A-B. To identify targets associated with MASLD, we intersected the 668 DEGs with disease-associated targets, yielding thirty common targets for further study, as shown in Fig. 6C. These targets were analyzed using the String 12.0 for PPI network analysis and visualised by Cytoscape 3.10.1. Fig. 6D illustrates a network with 30 nodes and 98 edges, where nodes like STEAP4, SLC13A5, NNMT, and SOCS2 were isolated without interactions. The node size and color intensity reflect their correlation with the drug's therapeutic mechanism. We calculated the Degree value of nodes using the CytoHubba plugin and reclassified the nodes with the M-CODE plugin, as shown in Supplementary Fig. 3C-D. GO enrichment and KEGG pathway analyses of core targets revealed their involvement in biological processes like nutrient response, lipid metabolism, and cellular responses to external stimuli (Fig. 6E). Key cellular components include pigment granules, melanosomes, endoplasmic reticulum chaperone complexes, and lipid droplets. Molecular functions involve unfolded protein binding and phosphatase binding. KEGG pathway analysis (Fig. 6F) highlighted pathways related to endoplasmic reticulum protein processing, non-alcoholic fatty liver disease, lipid metabolism, and atherosclerosis, with key signaling pathways including PPAR, PI3K/AKT, AMPK, and MAPK. Lastly, Autodock Vina was used to predict the binding modes of total anthraquinone components from CSEE—aloe emodin, rhein, edomin, chrysophanol, emodin 1-O-β-D-glucoside, emodin 8-O-β-D-glucoside, and physcion 8-O-β-D-glucoside—to key targets. Fifty docking simulations were performed, and the results were visualized in Fig. 6G-I, highlighting the complementary spatial structures and energy minimization of the ligand-receptor interactions.

3.7 CSEE alleviates HFD-induced hepatic steatosis in MASLD rats and hamsters by acting on lipid metabolism-related pathways

Based on the results from network pharmacology and high-throughput sequencing, we assessed the protein levels of AMPK, PPAR, PI3K/AKT, and their downstream lipid metabolism related proteins using Western blotting. Fig. 7A and 7B illustrates that a 10-week HFD significantly decreased the protein levels of p-AMPKα and p-ACC, while CSEE treatment increased their

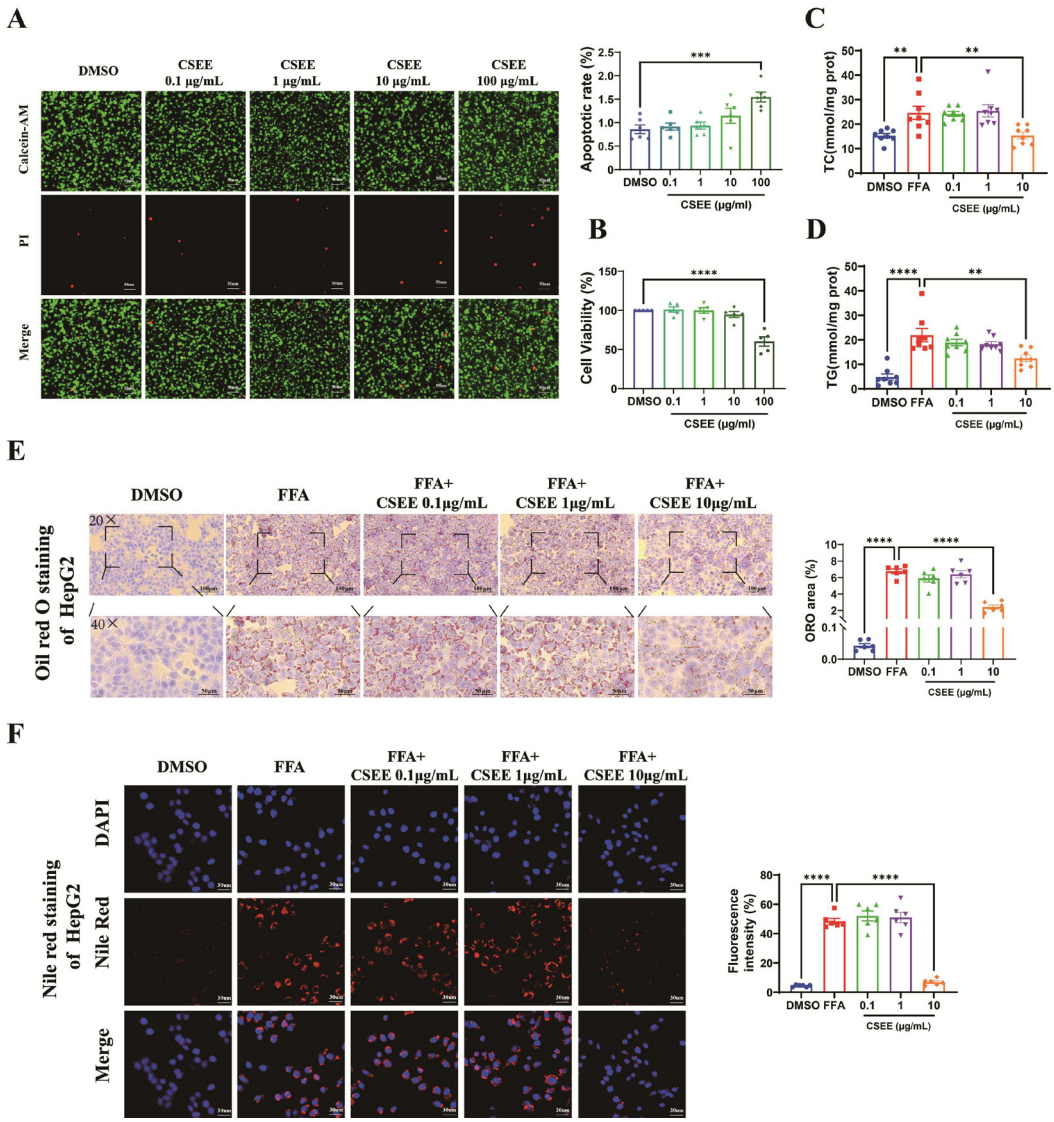

Fig. 5 Cassia seed ethanol extract (CSEE) prevents free fatty acid (FFA)-induced increase in lipid content in HepG2 cells

(A) Representative images of Calcein acetoxymethyl ester/Propidium Iodide (Calcein-AM/PI) staining in HepG2 cells after CSEE treatment. Scale bar: 50 μm, $N = 6$ per group. (B) Cell viability of HepG2 measured by cell counting kit-8 (CCK8). $N = 5$ per group. (C-D) The contents of (C) total cholesterol (TC) and (D) triglyceride (TG) in HepG2 after CSEE treatment. $N = 8$ per group. (E) Representative images of Oil Red O staining in HepG2. $N = 6$ per group. (F) Representative images of Nile Red staining in HepG2 cells. $N = 6$ per group. $^{**}P < 0.01$, $^{***}P < 0.001$, $^{****}P < 0.0001$. DMSO: Dimethyl sulfoxide.

phosphorylation levels. This suggests that CSEE activates the AMPK signaling pathway, which helps alleviate hepatic lipid deposition in both rats and hamsters with MASLD. AMPK, when activated, reduces hepatic fat synthesis by influencing fatty acid β-oxidation pathways, with CPT1A being a key enzyme in this process. In contrast, PPARγ and C/EBPα are crucial regulators of adipocyte formation. The data (Fig. 7A-B) show that, compared to the ND group, the HFD group had decreased levels of PPARα and CPT1A, and increased expression of C/EBPα and PPARγ. CSEE treatment, however, promoted PPARα and CPT1A expression while inhibiting liver C/EBPα and PPARγ levels. This indicates that CSEE enhances hepatic fatty acid oxidation and reduces adipocyte formation.

Additionally, the PI3K/AKT signaling pathway can promote fatty acid synthesis and lipid droplet formation through its effect on SREBP1c[27]. The results in Fig. 7A-B showed that hepatic steatosis inhibited the expression of PI3K P110 and p-AKT, whereas CSEE administration activated the PI3K P110/AKT pathway and inhibited hepatic lipid droplet formation.

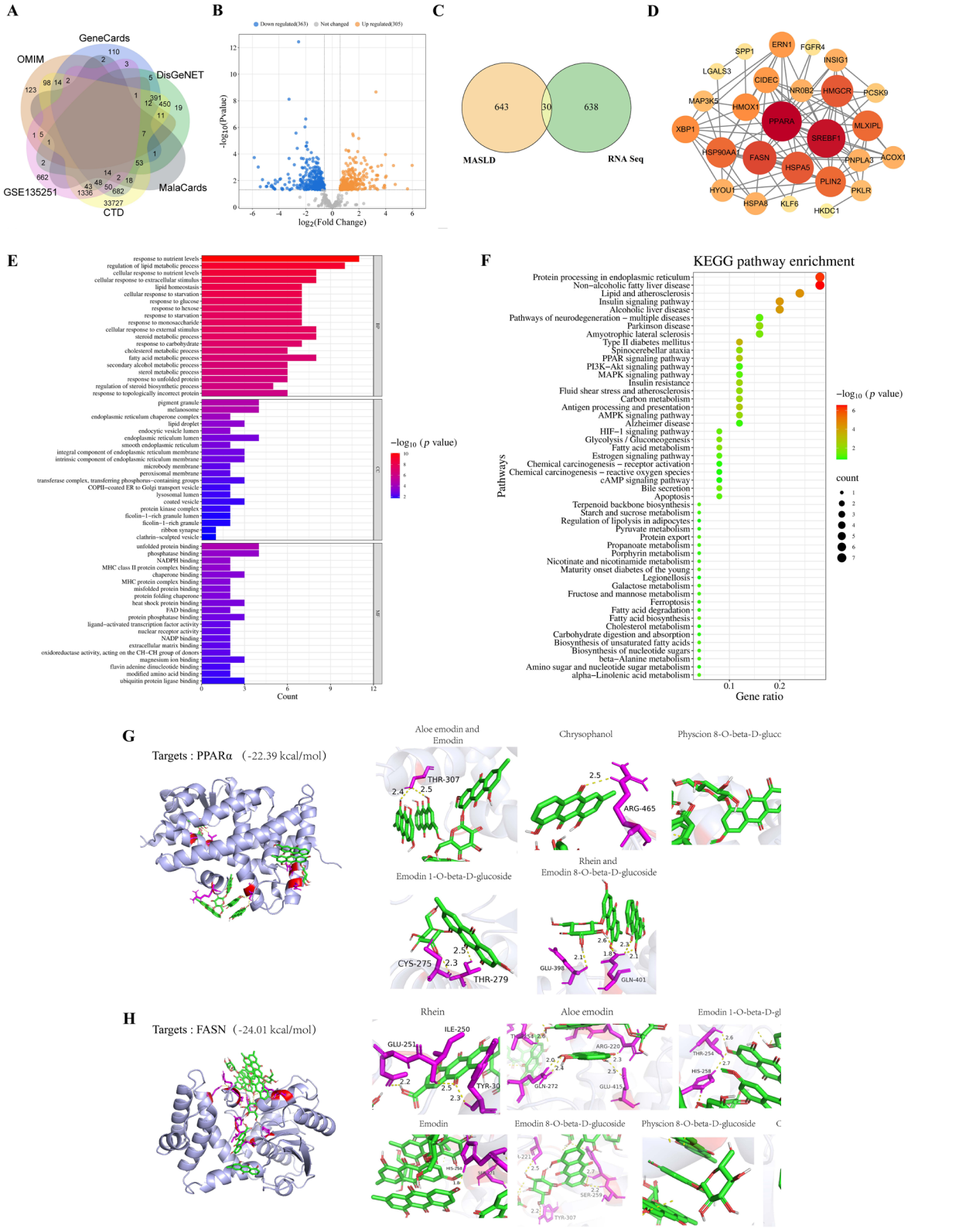
A
GeneCards
OMIM
DisGeNET
GSE135251
MalaCards
CTD
B
Down regulated(363)
Not changed
Up regulated(305)
-log10(Pvalue)
log2(Fold Change)
C
643
30
638
MASLD
RNA Seq
D
ERN1
FGFR4
SPP1
INSIG1
LGALS3
CIDEC
NR0B2
HMGCR
PCSK9
MAP3K5
HMOX1
PPARA
MLXIPL
XBP1
SREBF1
HSP90AA1
FASN
HSPA5
PNPLA3
ACOX1
PLIN2
HYOU1
PKLR
HSPA8
KLF6
HKDC1
E
response to nutrient levels
regulation of lipid metabolic process
cellular response to nutrient levels
cellular response to extracellular stimulus
lipid homeostasis
cellular response to starvation
response to glucose
response to hexose
response to starvation
response to monosaccharide
cellular response to external stimulus
steroid metabolic process
response to carbohydrate
cholesterol metabolic process
fatty acid metabolic process
secondary alcohol metabolic process
sterol metabolic process
response to unfolded protein
regulation of steroid biosynthetic process
response to topologically incorrect protein
pigment granule
melanosome
endoplasmic reticulum chaperone complex
lipid droplet
endocytic vesicle lumen
endoplasmic reticulum lumen
smooth endoplasmic reticulum
integral component of endoplasmic reticulum membrane
intrinsic component of endoplasmic reticulum membrane
microbody membrane
peroxisomal membrane
transferase complex, transferring phosphorus-containing groups
COPII-coated ER to Golgi transport vesicle
lysosomal lumen
coated vesicle
protein kinase complex
ficolin-1-rich granule lumen
ficolin-1-rich granule
ribbon synapse
clathrin-sculpted vesicle
unfolded protein binding
phosphatase binding
NADPH binding
MHC class II protein complex binding
chaperone binding
MHC protein complex binding
misfolded protein binding
protein folding chaperone
heat shock protein binding
FAD binding
protein phosphatase binding
ligand-activated transcription factor activity
nuclear receptor activity
NADP binding
extracellular matrix binding
oxidoreductase activity, acting on the CH-CH group of donors
magnesium ion binding
flavin adenine dinucleotide binding
modified amino acid binding
ubiquitin protein ligase binding
BP
CC
MF
Count
-log10 (p value)
F
KEGG pathway enrichment
Protein processing in endoplasmic reticulum
Non-alcoholic fatty liver disease
Lipid and atherosclerosis
Insulin signaling pathway
Alcoholic liver disease
Pathways of neurodegeneration - multiple diseases
Parkinson disease
Amyotrophic lateral sclerosis
Type II diabetes mellitus
Spinocerebellar ataxia
PPAR signaling pathway
PI3K-Akt signaling pathway
MAPK signaling pathway
Insulin resistance
Fluid shear stress and atherosclerosis
Carbon metabolism
Antigen processing and presentation
AMPK signaling pathway
Alzheimer disease
HIF-1 signaling pathway
Glycolysis / Gluconeogenesis
Fatty acid metabolism
Estrogen signaling pathway
Chemical carcinogenesis - receptor activation
Chemical carcinogenesis - reactive oxygen species
cAMP signaling pathway
Bile secretion
Apoptosis
Terpenoid backbone biosynthesis
Starch and sucrose metabolism
Regulation of lipolysis in adipocytes
Pyruvate metabolism
Protein export
Propanoate metabolism
Porphyrin metabolism
Nicotinate and nicotinamide metabolism
Maturity onset diabetes of the young
Legionellosis
Galactose metabolism
Fructose and mannose metabolism
Ferroptosis
Fatty acid degradation
Fatty acid biosynthesis
Cholesterol metabolism
Carbohydrate digestion and absorption
Biosynthesis of unsaturated fatty acids
Biosynthesis of nucleotide sugars
beta-Alanine metabolism
Amino sugar and nucleotide sugar metabolism
alpha-Linolenic acid metabolism
Pathways
Gene ratio
-log10 (p value)
count
G
Targets : PPARα (-22.39 kcal/mol)
Aloe emodin and Emodin
THR-307
Chrysophanol
ARG-465
Physcion 8-O-beta-D-glucc
Emodin 1-O-beta-D-glucoside
CYS-275
THR-279
Rhein and Emodin 8-O-beta-D-glucoside
GLU-398
GLN-401
H
Targets : FASN (-24.01 kcal/mol)
Rhein
GLU-251
ILE-250
TYR-30
Aloe emodin
ARG-220
GLN-272
GLU-415
Emodin 1-O-beta-D-gl
THR-254
HIS-258
Emodin
Emodin 8-O-beta-D-glucoside
Physcion 8-O-beta-D-glucoside

Continued.

Fig. 6 Continued.

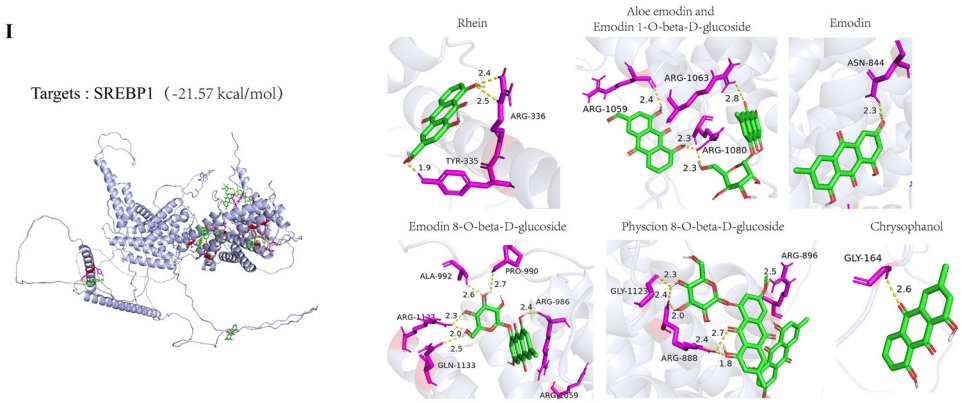

Fig. 6 Prediction and analysis of disease-drug targets

(A) Venn diagram of disease-related targets in five databases and GSE135251 dataset. (B) Volcano plot of differentially expressed genes (DEGs) in golden hamster livers between the high-fat-diet (HFD) group and the HFD + Cassia seed ethanol extract (CSEE) (250 mg/kg) group. (C) Venn diagram of DEGs. (D) Visualization of protein-protein interaction (PPI) network analysis. (E) Gene ontology (GO) enrichment analysis of targets (Top 20 terms of biological process, molecular function and cellular component). (F) Kyoto encyclopedia of genes and genomes (KEGG) enrichment analysis of targets (Top 50 pathways). (G-I) Molecular docking analysis of CSEE and (G) Peroxisome proliferator-activated receptor α (PPARα), (H) fatty acid synthase (FASN), and (I) sterol regulatory element-binding protein 1 (SREBP1).

We also examined the expression of genes involved in lipid synthesis and metabolism in the livers of rats and hamsters using qRT-PCR. The results presented in Figures 7C and 7D demonstrated that MASLD was associated with increased expression of lipid synthesis genes (PPARγ, CEBPA) and fatty acid uptake genes (FABP1, ACACA, ACACB, SREBF1, FASN, and ACLY), alongside a decrease in the expression of fatty acid oxidation-related genes (PPARα, CPT1A, and ACOX1). Treatment with CSEE reversed these HFD-induced changes in gene expression. Specifically, CSEE inhibited the upregulation of lipid synthesis and fatty acid uptake genes and promoted the expression of fatty acid oxidation genes. These results suggest that CSEE effectively suppresses lipid synthesis and fatty acid uptake while enhancing fatty acid oxidation, thereby contributing to the amelioration of MASLD.

3.8 Inhibition of the AMPK, PPARα, and PI3K/AKT signaling pathways reversed the lipid-lowering effect of CSEE

To further validate the roles of the AMPK, PPARα, and PI3K/AKT signaling pathways in the treatment of MASLD with CSEE, we performed *in vitro* experiments using specific small molecule inhibitors. The results from biochemical assays (Fig. 8A and 8B) demonstrated that CSEE effectively reduced the FFA-induced elevations in TC and TG levels. However, these beneficial effects of CSEE were reversed when cells were co-treated with a mixture of inhibitors targeting AMPK, PPARα, and PI3K/AKT pathways. Additionally, Oil Red O staining (Fig. 8C) and Nile Red staining (Fig. 8D) corroborated these findings, showing that the reduction in intracellular lipid droplets induced by CSEE was mitigated in the presence of the inhibitors. These results confirm that the therapeutic effects of CSEE are, at least in part, mediated through the AMPK, PPARα, and PI3K/AKT signaling pathways.

4 Discussion

With the global shift towards modern lifestyles, the prevalence of metabolism-related diseases has risen sharply, making MASLD one of the most common chronic liver conditions. MASLD is closely linked to metabolic syndrome, T2DM, and hyperlipidemia. Clinically, MASLD is characterized by excessive hepatic lipid accumulation, presenting as a relatively benign liver condition in its early stages. However, if left untreated or unmanaged, it can progress to more severe forms such as MASH, liver fibrosis, and potentially liver cancer, leading to significant patient suffering and financial burden.

Current treatments options for MASLD primarily involve lifestyle interventions, but long-term adherence to these interventions is often poor. Consequently, there is a critical need for effective therapeutic agents. Our research group is focused on the developing therapeutic agents derived from herbal extracts for MASLD treatment. Cassia seed, a commonly used medicinal herb in traditional Chinese medicine, is known for its benefits in liver health and vision enhancement. However, the diverse components of traditional Chinese medicine can have varying pharmacological effects depending on the extraction methods used, and the specific mechanisms of Cassia seed extract in treating MASLD have not been fully elucidated. In our study, we selected Cassia seed extract, prepared with 90% ethanol and purified through macroporous resin, as the subject of investigation to explore its pharmacological effects on MASLD.

In our study, we utilized network pharmacology and high-throughput sequencing to identify and validate the therapeutic targets of CSEE for treating MASLD. The analysis suggested that CSEE impacts multiple lipid metabolism-related signaling pathways, including PPAR, PI3K/AKT, and AMPK. To ensure the reliability and accuracy of our findings, and to establish a dosage reference for clinical use, we conducted experiments in both rats and hamsters. Our results demonstrated that CSEE effectively alleviated hyperlipidemia and hepatic steatosis induced by MASLD in both rats and hamsters. Notably, the required therapeutic dose

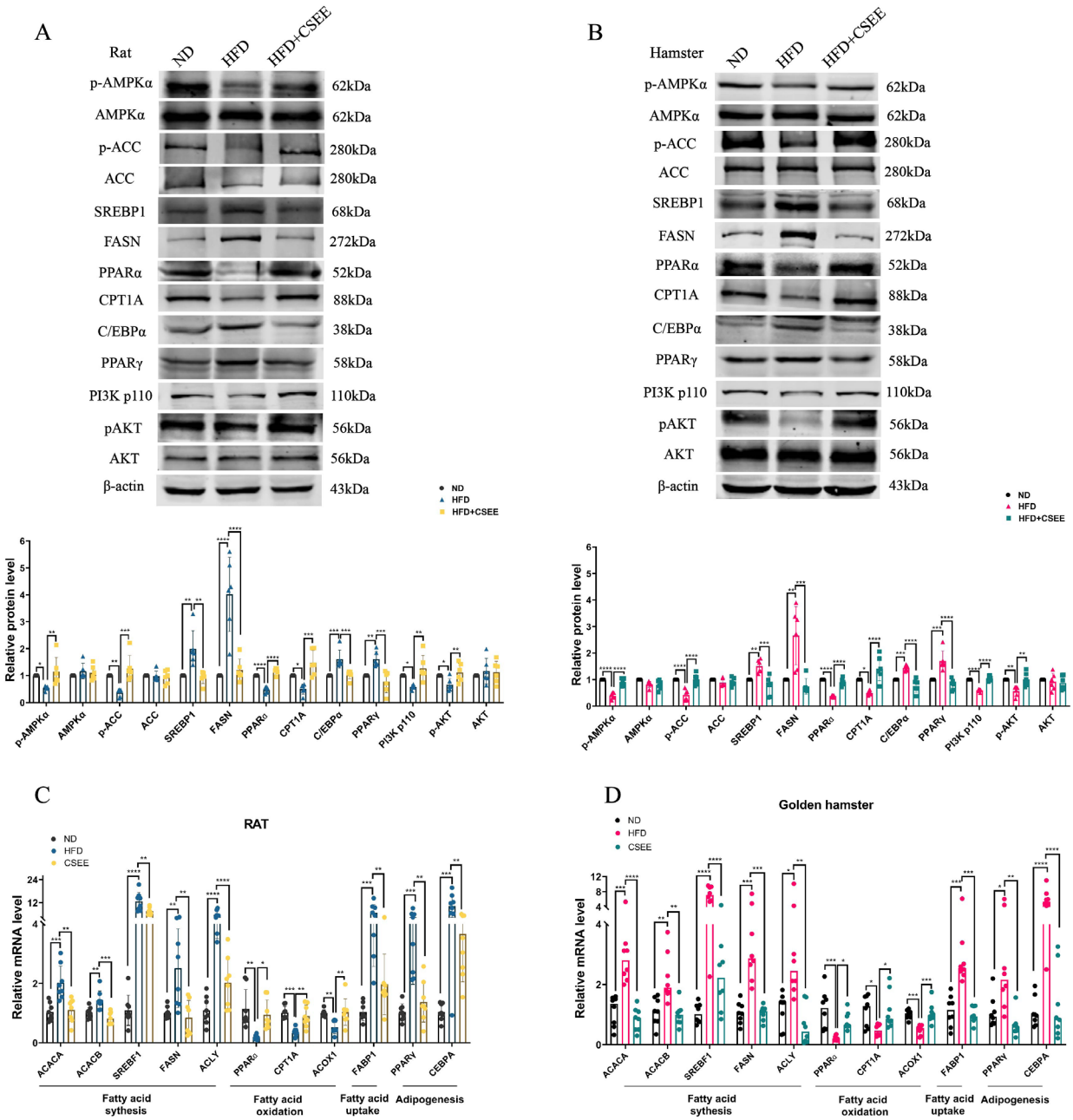

Fig. 7 Cassia seed ethanol extract (CSEE) alleviates high-fat-diet (HFD)-induced hepatic steatosis by activating multiple signalling pathways

(A-B) Relative protein levels of the AMP-activated protein kinase (AMPK), peroxisome proliferator-activated receptor (PPAR), and phosphoinositide 3-kinase (PI3K)/AKT signalling pathways in (A) rat and (B) hamster livers, determined by Western blotting. $N = 6$ per group. (C-D) mRNA levels of the genes related to fatty acid synthesis, oxidation, uptake, and adipogenesis, as quantified by qRT-PCR. $N = 8$ per group. $^{*}P < 0.05$, $^{**}P < 0.01$, $^{***}P < 0.001$, $^{****}P < 0.0001$. ND: Normal diet.

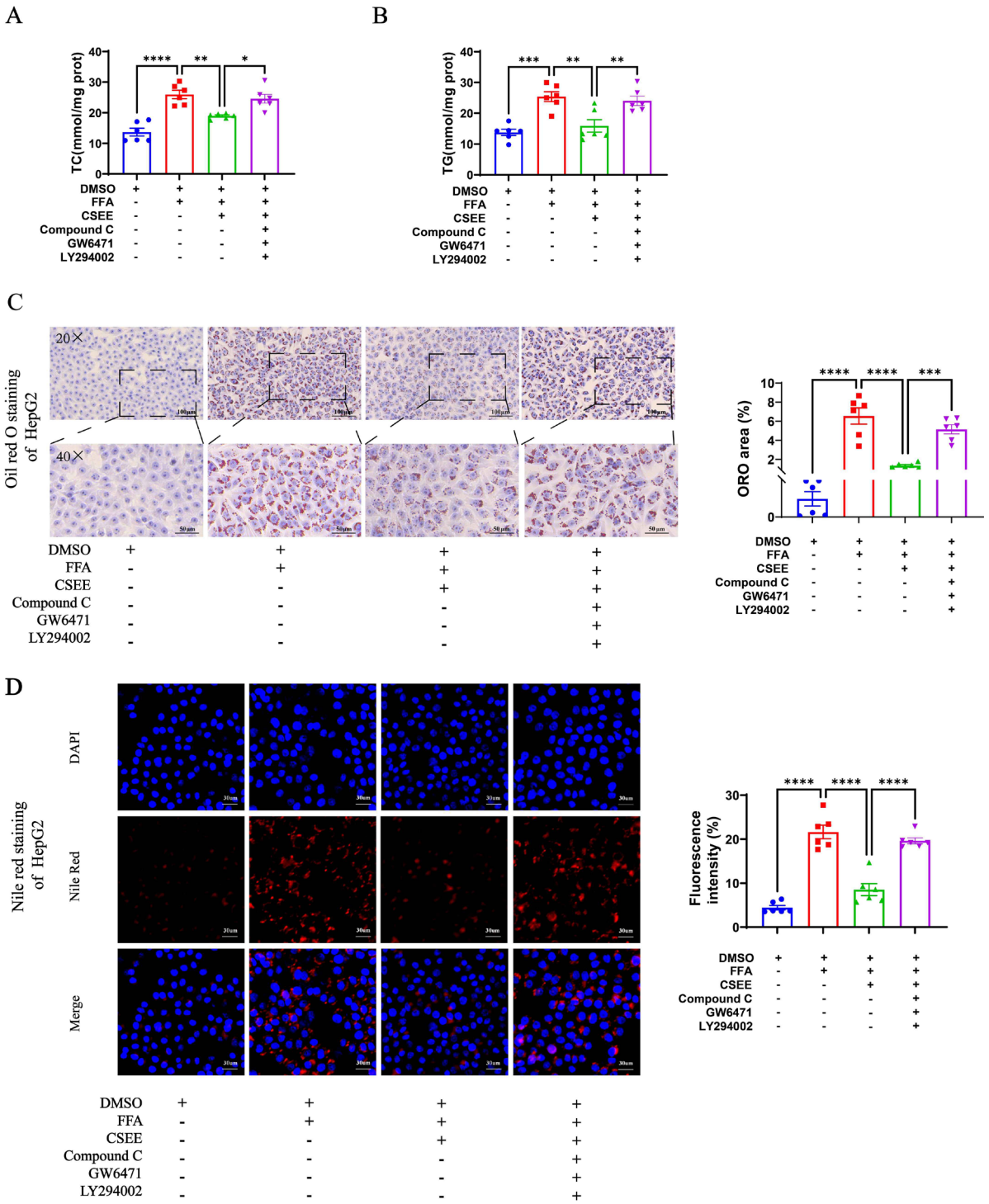

Fig. 8 Inhibition of AMP-activated protein kinase (AMPK), peroxisome proliferator-activated receptorα (PPARα), and phosphoinositide 3-kinase (PI3K)/AKT reverses the beneficial effects of Cassia seed ethanol extract (CSEE) on lipid contents

(A-B) The contents of (A) total cholesterol (TC) and (B) triglyceride (TG) in HepG2 cells. $N = 6$ per group. (C) Representative images of Oil Red O staining in HepG2 cells. $N = 6$ per group. (D) Representative images of Nile Red staining in HepG2 cells. $N = 6$ per group. $^{*}P < 0.05$, $^{**}P < 0.01$, $^{***}P < 0.001$, $^{****}P < 0.0001$. DMSO: Dimethyl sulfoxide. FFA: Free fatty acid.

of CSEE for hamsters was higher compared to rats. This difference is likely due to hamsters' greater sensitivity to high-fat diets and their lipid metabolism pattern, which more closely resembles that of humans compared to rats. Hamsters possess cholesteryl ester transfer protein (CETP), a protein absent in rats, which contributes to their lipid metabolism dynamics[28]. This insight is crucial for optimizing dosage and treatment strategies in future clinical applications.

Our research clarified that CSEE primarily mitigates hepatic lipid deposition by modulating lipid metabolism-related pathways, including AMPK, PPAR, and PI3K/AKT. AMPK, a crucial metabolic regulator, influences various tissues and maintains lipid homeostasis by regulating fatty acid and cholesterol synthesis[29]. MASLD is characterized by reduced AMPK activity in the liver. Our findings show that CSEE enhances the phosphorylation of AMPK and ACC, thereby activating the AMPK signaling pathway and improving lipid metabolism in both rats and hamsters with MASLD[30]. CSEE also reduces the levels of SREBP1 and FASN, key factors in lipogenesis downstream of AMPK. This suggests that AMPK activation is a significant mechanism through which CSEE alleviates hepatic lipid metabolism disorders. The development of small molecule agonists for activating AMPK is currently underway, but their safety and efficacy needs verification and validations in clinical trials[31].

PPARα, an essential nuclear receptor, primarily regulates the β-oxidation of fatty acids in mitochondria, thereby maintaining hepatic lipid metabolic homeostasis. Pemafibrate, a PPARα agonist, is frequently used to treat hyperlipidemia and has been shown to enhance liver function and reduce liver fibrosis in patients with MASLD[32]. PPARα agonists reduce lipid accumulation by targeting CPT1A, a mitochondrial membrane protein crucial for converting long-chain fatty acyl coenzyme A molecules into acyl carnitine molecules[33]. Our experimental results indicate that CSEE enhances CPT1A protein levels by activating PPARα, which promotes hepatic fatty acid oxidation and reduces lipid deposition. Additionally, PPARα has been reported to regulate hepatic energy metabolism by increasing lipocalin production, which in turn activates AMPK[34]. In contrast, PPARγ, another isoform of PPAR, is critical for lipid synthesis, metabolism, and insulin homeostasis[35]. PPARγ, along with C/EBPα, plays a pivotal role in the early stages of adipogenesis. C/EBPα binds to the promoter of PPARγ, inducing the expression of PPARγ isoform 2, which enhances adipogenesis and promotes hepatic steatosis[36]. Our findings show that CSEE can counteract the HFD-induced elevation of PPARγ and C/EBPα protein levels, thereby mitigating hepatic fat deposition.

Related studies have shown that AKT in the liver is primarily activated by PI3K p110α in metabolic diseases, and selective inhibition of PI3K p110α leads to increased hepatic lipid deposition[37]. Our results indicate that CSEE enhances the protein levels of PI3K p110 and p-AKT, thereby activating the PI3K P110/AKT signalling pathway. Additionally, the AKT, PPARα, and AMPK signalling pathways interact to reduce lipid accumulation and oxidative stress in the liver[38]. These findings suggest that the interplay among different signaling pathways plays a crucial role in the treatment of MASLD. *In vitro* experiments further confirmed that the protective effect of CSEE are reversed when these key metabolic pathways were inhibited.

Due to the complexity of metabolic disease pathogenesis, combination therapies are often used to improve patient outcomes. Our study demonstrated that CSEE can exert therapeutic effects through the modulation of multiple signaling pathways, providing a strong rationale for its use in treating MASLD. However, network pharmacology, while valuable, has its limitations. It relies on various analytical tools and databases, which may vary in focus and completeness, leading to potential biases. Additionally, the pharmacological properties of herbal medicines can differ based on their source, and network pharmacology alone may not fully account for these variations. Therefore, predictions made by network pharmacology should be supplemented with experimental validation. Our research shows that CSEE has a beneficial effect on HFD-induced MASLD, improving liver weight and morphology, and reducing intracellular lipid accumulation in experimental animals. As a herbal extract, CSEE's effects may vary depending on the specific components extracted.

In this study, cassia seed was extracted using 70% ethanol and further processed with 90% ethanol, resulting in an extract rich in lipid-soluble anthraquinones. These anthraquinones may be crucial in MASLD treatment, suggesting that exploring other anthraquinone-containing plants could also be promising. Overall, the findings from this study advance the potential of herbal extracts as treatments for metabolic disorders and provide a foundation for future clinical treatment of CSEE.

5 Conclusion

In summary, this study demonstrated the beneficial effect of CSEE in combating MASLD. We confirmed that We confirmed that CSEE exerts its therapeutic effects through the activation of multiple signaling pathways, including AMPK, PPARα, and PI3K/AKT. These pathways play crucial roles in regulating lipid metabolism and reducing hepatic lipid accumulation.

Author contributions

All authors read and approved the manuscript. Conception and design: Du Z M. Administrative support: Du Z M. Research, data collection and analysis: Li W, Wang J, Yang Y L, Duan C L, Shao B,

Zhang M X, Wang J P and Li P F. Preparation of manuscripts: Li W, Wang J and Yang Y L. Review of manuscripts: Du Z M, Yuan Y, Zhang Y, Ji H Y and Li X D.

Source of funding

This research was funded by National Natural Science Foundation of China (grant number 82073838 and 82273917).

Conflict of interest

The authors have no relevant financial or non-financial interests to disclose.

Ethical approval

The animal protocols were approved by the Ethics Committee of the Second Affiliated Hospital of Harbin Medical University (SYDW2019-258).

Data availability statement

Data used to support the findings of this study are available from the corresponding author upon request.

References

[1] Man S, Deng Y, Ma Y, *et al.* Prevalence of liver steatosis and fibrosis in the general population and various high-risk populations: a nationwide study with 5.7 million adults in China. Gastroenterology, 2023; 165(4): 1025-1040.
[2] Le M, Le D, Baez T, *et al.* Global incidence of non-alcoholic fatty liver disease: A systematic review and meta-analysis of 63 studies and 1,201,807 persons. J Hepatol, 2023; 79(2): 287-295.
[3] Riazi K, Azhari H, Charette J, *et al.* The prevalence and incidence of NAFLD worldwide: a systematic review and meta-analysis. Lancet Gastroenterol Hepatol, 2022; 7(9): 851-861.
[4] Qian Y, Che Z, Fu C, *et al.* Study on the association between dietary quality and overweight/obesity of Han nationality with cold in Yunnan plateau by DBI-16 - a study based on a multi-ethnic cohort in China. Diabetes Metab Syndr Obes, 2023; 16: 2311-2327.
[5] Assy N, Kaita K, Mymin D, *et al.* Fatty infiltration of liver in hyperlipidemic patients. Dig Dis Sci, 2000; 45(10): 1929-1934.
[6] Li G, Peng Y, Chen Z, *et al.* Bidirectional association between hypertension and NAFLD: a systematic review and meta-analysis of observational studies. Int J Endocrinol, 2022; 2022: 8463640.
[7] Ramanathan R, Patwa S, Ali A, *et al.* Thyroid hormone and mitochondrial dysfunction: therapeutic implications for metabolic dysfunction-associated steatotic liver disease (MASLD). Cells 2023; 12(24): 2806.
[8] Semmler G, Balcar L, Wernly S, *et al.* Insulin resistance and central obesity determine hepatic steatosis and explain cardiovascular risk in steatotic liver disease. Front Endocrinol (Lausanne), 2023; 14: 1244405.
[9] Liu S, Liu Y, Wan B, *et al.* Association between vitamin D status and non-alcoholic fatty liver disease: a population-based study. J Nutr Sci Vitaminol (Tokyo), 2019; 65: 303-308.
[10] Zhang J, Wang Q H, Miao B B, *et al.* Liver transcriptome analysis reveal the metabolic and apoptotic responses of Trachinotus ovatus under acute cold stress. Fish Shellfish Immunol, 2024; 148: 109476.
[11] Teng T, Sun G, Ding H *et al.* Characteristics of glucose and lipid metabolism and the interaction between gut microbiota and colonic mucosal immunity in pigs during cold exposure. J Anim Sci Biotechnol, 2023; 14(1): 84.
[12] Haase C, Lopes S, Olsen A, *et al.* Weight loss and risk reduction of obesity-related outcomes in 0.5 million people: evidence from a UK primary care database. Int J Obes (Lond), 2021; 45(6): 1249-1258.
[13] Sookoian S, Pirola C J. Resmetirom for treatment of MASH. Cell, 2024; 187(12): 2897-2897.e1.
[14] Chen Y, Chen X, Yang X, *et al.* Cassiae Semen: A comprehensive review of botany, traditional use, phytochemistry, pharmacology, toxicity, and quality control. J Ethnopharmacol, 2023; 306: 116199.
[15] Ju M, Kim H, Choi J, *et al.* Cassiae semen, a seed of Cassia obtusifolia, has neuroprotective effects in Parkinson's disease models. Food Chem Toxicol, 2010; 48(8-9): 2037-2044.
[16] Kim S, Ban J, Kang H, *et al.* Anti-apoptotic effect of chrysophanol isolated from Cassia tora seed extract on blue-light-induced a2e-loaded human retinal pigment epithelial cells. Int J Mol Sci, 2023; 24(7): 6676.
[17] Patil U, Saraf S, Dixit V. Hypolipidemic activity of seeds of Cassia tora Linn. J Ethnopharmacol, 2004; 90(2-3): 249-252.
[18] Shih Y, Chen F, Wang L,*et al.* Discovery and study of novel antihypertensive peptides derived from Cassia obtusifolia seeds. J Agric Food Chem, 2019; 67(28): 7810-7820.
[19] Wang Q, Zhou J, Xiang Z, *et al.* Anti-diabetic and renoprotective effects of Cassiae Semen extract in the streptozotocin-induced diabetic rats. J Ethnopharmacol, 2019; 239: 111904.
[20] Zhou F, Ding M, Gu Y, *et al.* Aurantio-obtusin attenuates non-alcoholic fatty liver disease through AMPK-mediated autophagy and fatty acid oxidation pathways. Front Pharmacol, 2021; 12: 826628.
[21] Albillos A, de Gottardi A, Rescigno M. The gut-liver axis in liver disease: Pathophysiological basis for therapy. J Hepatol, 2020; 72(3): 558-577.
[22] Luo H, Wu H, Wang L, *et al.* Hepatoprotective effects of Cassiae Semen on mice with non-alcoholic fatty liver disease based on gut microbiota. Commun Biol, 2021; 4(1): 1357.
[23] Lei N, Song H, Zeng L, *et al.* Persistent lipid accumulation leads to persistent exacerbation of endoplasmic reticulum stress and inflammation in progressive NASH *via* the IRE1alpha/TRAF2 complex. Molecules, 2023; 28(7): 3185.
[24] Li F, Jiang M, Ma M, *et al.* Anthelmintics nitazoxanide protects

against experimental hyperlipidemia and hepatic steatosis in hamsters and mice. Acta Pharm Sin B, 2022; 12(3): 1322-1338.
[25] Song S, Lai J, Wong G, *et al.* Can we use old NAFLD data under the new MASLD definition? J Hepatol, 2024; 80(2): e54-e56.
[26] Eslam M, Newsome P, Sarin S, *et al.* A new definition for metabolic dysfunction-associated fatty liver disease: An international expert consensus statement. J Hepatol, 2020; 73(1): 202-209.
[27] Liu J, Wang X, Zhu Y, *et al.* Theabrownin from dark tea ameliorates insulin resistance *via* attenuating oxidative stress and modulating IRS-1/PI3K/Akt pathway in HepG2 cells. Nutrients, 2023; 15(18): 3862.
[28] Dong Z, Shi H, Zhao M, *et al.* Loss of LCAT activity in the golden Syrian hamster elicits pro-atherogenic dyslipidemia and enhanced atherosclerosis. Metabolism, 2018; 83: 245-255.
[29] Atteia H, AlFaris N, Alshammari G, *et al.* The hepatic antisteatosis effect of xanthohumol in high-fat diet-fed rats entails activation of AMPK as a possible protective mechanism. Foods, 2023; 12(23): 4214.
[30] Fang C, Pan J, Qu N, *et al.* The AMPK pathway in fatty liver disease. Front Physiol, 2022; 13: 970292.
[31] Steinberg G, Carling D. AMP-activated protein kinase: the current landscape for drug development. Nat Rev Drug Discov, 2019; 18(7): 527-551.
[32] Katsuyama H, Yanai H, Adachi H, *et al.* A significant effect of pemafibrate on hepatic steatosis and fibrosis indexes in patients with hypertriglyceridemia. Gastroenterology Res, 2023; 16(4): 240-243.
[33] Nakamura M, Yudell B, Loor J. Regulation of energy metabolism by long-chain fatty acids. Prog Lipid Res, 2014; 53: 124-144.
[34] Yanai H, Yoshida H. Beneficial effects of adiponectin on glucose and lipid metabolism and atherosclerotic progression: mechanisms and perspectives. Int J Mol Sci, 2019; 20(5): 1190.
[35] Habtemichael E, Li D, Camporez J, *et al.* Insulin-stimulated endoproteolytic TUG cleavage links energy expenditure with glucose uptake. Nat Metab, 2021; 3(3): 378-393.
[36] Leem Y, Bae J, Jeong H, *et al.* PRMT7 deficiency enhances adipogenesis through modulation of C/EBP-beta. Biochem Biophys Res Commun, 2019; 517(3): 484-490.
[37] Sopasakis V, Liu P, Suzuki R, *et al.* Specific roles of the p110alpha isoform of phosphatidylinsositol 3-kinase in hepatic insulin signaling and metabolic regulation. Cell Metab, 2010; 11(3): 220-230.
[38] Tamilmani P, Sathibabu Uddandrao V, Chandrasekaran P, *et al.* Linalool attenuates lipid accumulation and oxidative stress in metabolic dysfunction-associated steatotic liver disease *via* Sirt1/Akt/PPRA-alpha/AMPK and Nrf-2/HO-1 signaling pathways. Clin Res Hepatol Gastroenterol, 2023; 47(10): 102231.